P6.20

# TWO MODIS AEROSOL PRODUCTS OVER OCEAN ON THE TERRA AND AQUA CERES SSF DATASETS

Alexander Ignatov*[1], Patrick Minnis[2], Norman Loeb[3], Bruce Wielicki[2], Walter Miller[4], Sunny Sun-Mack[4], Didier Tanré[5], Lorraine Remer[6], Istvan Laszlo[1], Erika Geier[2]

[1]*NOAA/NESDIS/ORA, Camp Springs, MD, USA*
[2]*NASA/LaRC, Atmospheric Sciences, VA, USA*
[3]*Center for Atmospheric Sciences, Hampton Univ., Hampton, VA, USA*
[4]*Science Applications International Corporation, Hampton, VA, USA*
[5]*Lab. d'Optique Atmospherique, Univ. des Sciences et Technologies de Lille, Villenueve d'Asq, France*
[6]*NASA/GSFC, Greenbelt, MD, USA*

## 1. INTRODUCTION

Aerosols have an important, yet somewhat uncertain, impact on the Earth's radiation budget and climate. Determining that impact on the climate record requires consistent measurements of aerosol properties and radiative fluxes. Three satellites, the Tropical Rainfall Measuring Mission (TRMM), *Terra*, and *Aqua* (launched in November 1997, December 1999, and May 2002, respectively) carry a total of five Clouds and the Earth's Radiant Energy System (CERES) instruments, to measure the radiant energy exchange on Earth (Wielicki et al. 1996). The TRMM satellite carries the CERES proto-flight model (PFM); *Terra* carries flight models 1 and 2 (FM1-2); and *Aqua* carries flight models 3 and 4 (FM3-4).

The Single Scanner Footprint (SSF) products (Geier et al. 2003) combine the CERES data with cloud and aerosol retrievals from the Visible and Infra-Red Scanner (VIRS) on TRMM, and MODerate resolution Imaging Spectroradiometer (MODIS) on *Terra* and *Aqua*. The spatial resolution is ~2 km at nadir for VIRS, and 0.25-1 km for MODIS. The SSF retains the mean and standard deviation of the imager pixel radiances and cloud/aerosol retrievals separately for the clear and cloudy portions of every CERES field-of-view (FOV). The spatial resolution for CERES (equivalent diameter at nadir) is ~10 km on TRMM, and ~20 km on *Terra* and *Aqua*.

Over ocean, two aerosol products are reported on the *Terra* and *Aqua* CERES SSFs. Both are derived from MODIS, but using different sampling and aerosol algorithms. This study briefly summarizes these products, and compares using 2 weeks of global *Terra* data from 15-21 December 2000, and 1-7 June 2001. A more full and detailed description of the CERES SSF aerosol production for the *Terra* and *Aqua* is found in Ignatov et al. (2004a).

On the TRMM SSF, only one aerosol product is available. This product is documented in Ignatov et al. (2004b).

* *Corresponding author address*: Alexander Ignatov, E/RA2, Rm.603, WWB, NOAA, 5200 Auth Rd., Camp Springs, MD 20746-4304; e-mail: Alex.Ignatov@noaa.gov

## 2. THE M- AND A-AEROSOL PRODUCTS

The *primary*, M, aerosol product on the CERES SSF is generated by subsetting and remapping the MOD04 granules onto CERES footprints. The MOD04 product uses sophisticated cloud screening and aerosol retrieval algorithms developed by the MODIS cloud and aerosol groups (Ackerman et al. 1998; Tanré et al. 1997; Levy et al. 2002; Martins et al. 2002; Remer et al. 2004). In this study, only two M- aerosol optical depths (AOD), $\tau_{M1}$ and $\tau_{M2}$, are used reported at the centroid wavelengths of MODIS bands 1 ($\lambda_1$=0.644 μm) and 6 ($\lambda_2$=1.632 μm).

The *secondary* A-product uses different glint and cloud screening criteria (Trepte et al. 1999; Minnis et al 2004; summarized in Ignatov et al. 2004b), and a simpler (Advanced Very High Resolution Radiometer, AVHRR-like) 3rd generation NESDIS aerosol algorithm currently employed operationally with AVHRR/3 on NOAA-16 and -17 platforms (Ignatov and Stowe 2002a; Ignatov et al. 2004c). Two AODs, $\tau_{A1}$(0.630 μm) and $\tau_{A2}$(1.610 μm), are derived from MODIS bands 1 and 6 using single-channel algorithms, and reported at the wavelengths representative of band centers for a generic AVHRR or VIRS sensor. Using a standard set of reference wavelengths ensures compatibility of the respective A-products derived from a variety of sensors (AVHRR, VIRS, and MODIS) flown onboard different platforms (NOAA, TRMM, *Terra* and *Aqua*). Cross-platform differences in the A-products, if observed, are then due to either different sampling of aerosol pixels (different cloud/glint screening, and different domains of the sun-view-scatter-glint geometry resulting from a different orbit configuration), or different radiometric performance of the sensors, or both. The respective Ångström exponents are derived from either M- or A-AODs as $\alpha=-\ln(\tau_1/\tau_2)/\ln(\lambda_1/\lambda_2)$.

The availability of the two aerosol products on the CERES SSF side-by-side is helpful to place long-term time series of the heritage A-products from AVHRR (20+ years) and VIRS (6+ years) in context of more accurate M-aerosol retrievals, and to quickly assess the improvements provided by the multi-channel MODIS. Ultimately, these analyses provide a useful insight into the current status of aerosol retrievals from space, and serve to highlight and prioritize outstanding issues.

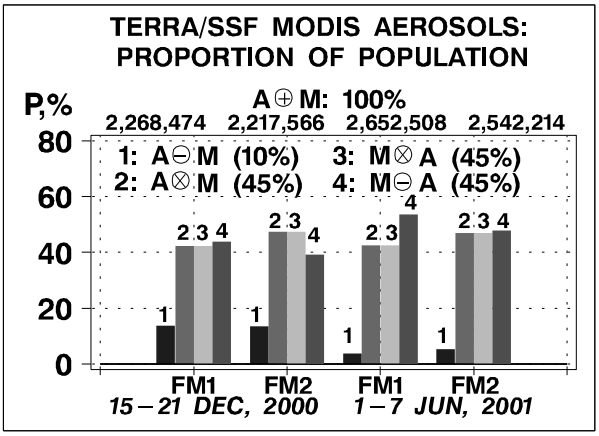


**Fig.1.** Count of CERES footprints with valid aerosol retrievals in four datasets: December 2000 and June 2001, FM1 and FM2. The union sample, M⊕A (defined as 100%) consists of all FOVs in which either M- or A-aerosol retrievals are available. (Corresponding counts of CERES FOVs are listed in the top of Figure.) The intersection sample, M⊗A (≡A⊗M; ~45% of the union sample, on average) consists of all FOVs in which both M- and A-aerosol retrievals are available. The M-complement, M⊖A (~45% of the union sample, on average) consists of all FOVs in which the M-retrievals are available but the A-retrievals are not. The A-complement, A⊖M (~10% of the union sample, on average) consists of all FOVs in which the A-retrievals are available but the M-retrievals are not.

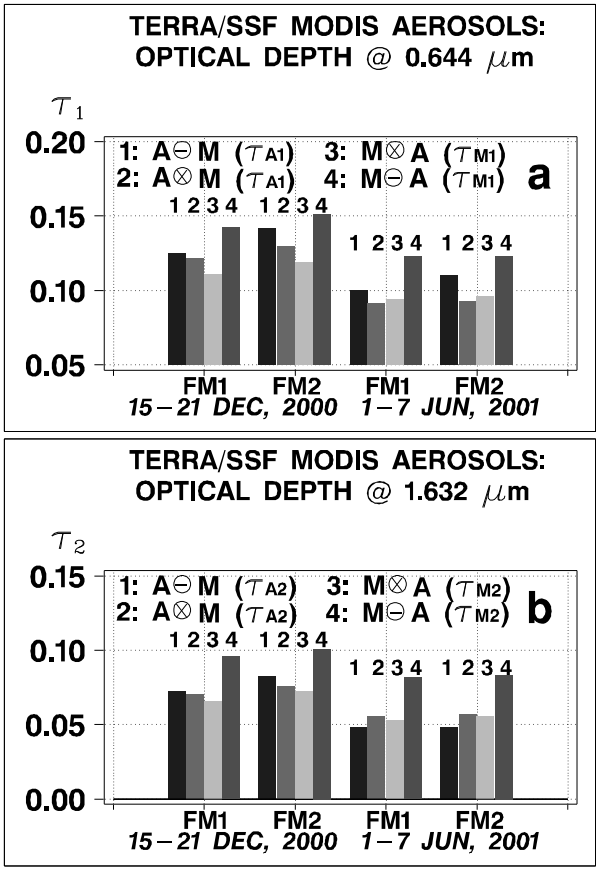


**Fig.2.** Average statistics of aerosol retrievals in December 2000 and June 2001, FM1 and FM2 datasets. (Samples are defined in caption to Fig.1.)

## 3. COMPARISON OF M- AND A-PRODUCTS

Differences between the M- and A-products on the CERES SSFs are expected due to: (1) different sampling (cloud and glint screening); (2) different aerosol algorithms (including different treatment of aerosol microphysics, Rayleigh scattering, gaseous absorption, surface reflectance, radiative transfer model used to generate the look-up tables, and numerical inversion methods); (3) different propagation of data errors (resulting from sensor calibration and other radiometric uncertainties) in the M- and A-products.

Below, the two products are compared and their observed differences discussed in terms of the potential error sources, (1), (2), and (3).

### *3.1 Defining the M- and A-(sub) samples*

Statistics superimposed in Fig.1 show that there are from ~2.2–2.3 million CERES footprints with at least one M- or A- aerosol retrieval in December 2000, and from 2.5–2.6 million in June 2001. Hereafter, these datasets are referred to as the MA union samples, or M⊕A≡A⊕M, and are considered =100%, by definition. In a union sample, there are some CERES FOVs in which both M- and A-product retrievals are available. They form a sub-sample that is termed the MA intersection: M⊗A≡A⊗M. Figure 1 shows that the MA intersection accounts for ~45% of the union sample. In some CERES FOVs, only the M retrievals are available (but the A-retrievals are not); this subset is called the M complement, or M⊖A. Likewise, the footprints having only A-retrievals (but not M-retrievals) form the A complement, or A⊖M. The M and A complements account for another ~45% and ~10% of the union sample, respectively. The M and A complements highlight the effect of different sampling procedures (glint screening and cloud clearing) on the retrievals, whereas the MA intersection can be used to examine the effect of the aerosol algorithm differences.

The MA intersection and the M and A complements divide the union sample into three non-overlapping sub-samples from which other subsets can be constructed. In particular, the full M sample (referred to as the "M-product") comprises all footprints with valid M retrievals, regardless of A-product availability. It is thus defined as a union of the MA intersection and the M complement: M≡(M⊗A)⊕(M⊖A), and accounts for ~90% of the union sample. Likewise, the full A sample (the "A-product") is a union of the MA intersection and A complement, M≡(M⊗A)⊕(A⊖M), and accounts for only ~55% of the union sample. The large difference between the M and A samples mainly results from excluding the solar side of the orbit in the A-product processing, in addition to the glint angle screening <40° used in both products.

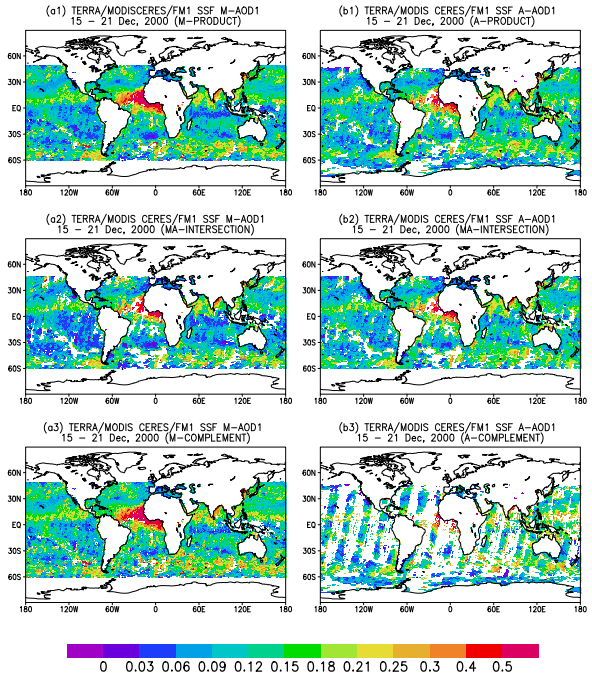


**Fig.3.** Mapping (a) $\tau_{1M}$- and (b) $\tau_{1A}$-products for different sub-samples (data of *Terra* CERES SSF FM1, December 2000): (1) full product [M≡(M⊗A)⊕(M⊖A), A≡(M⊗A)⊕(A⊖M)]; (2) MA-intersection (M⊗A); (3) M- and A-supplements [(M⊖A) and (A⊖M)].

### *3.2 Global Aerosol Distribution and Statistics*

Figure 2 summarizes the average statistics of the M- and A-τ for December 2000 and June 2001 for FM1 and FM2. An example of global distribution of $\tau_1$ from which Fig.2 was derived is shown in Fig.3 for December 2000, FM1 dataset. For each dataset, we provide two M-statistics (derived from Figs.3a2 and a3), and two A-statistics (derived from Figs.3b2 and b3). Statistics for the M- (Fig.3a1) and A-products (Fig.3b1) fall between their intersection and complement counterparts and therefore are not shown.

The following observations emerge from Figs.2-3:

(A) The M complement (cluster "4") clearly stands out as different from the MA intersection (cluster "3"). The only difference between clusters "4" and "3" is sampling as the M-aerosol algorithm is the same here.

(B) Sampling-induced differences in the A-product (between the MA intersection and the A complement; clusters "1" and "2") are generally smaller than the sample-induced M differences.

(C) AOD is lower in June 2001 compared to December 2000. This difference is statistically significant in both bands 1 and 6, in both SSF datasets (FM1 and FM2), and in both products (M- and A-).

(D) Aerosol algorithm-induced global differences between the M and A retrievals in the MA intersection (cluster "2" vs. "3") are within $\sim(4\pm5)\times10^{-3}$ for $\tau_1$, $\sim(3\pm1)\times10^{-3}$ for $\tau_2$, and $\sim(1\pm1)\times10^{-1}$ for α.

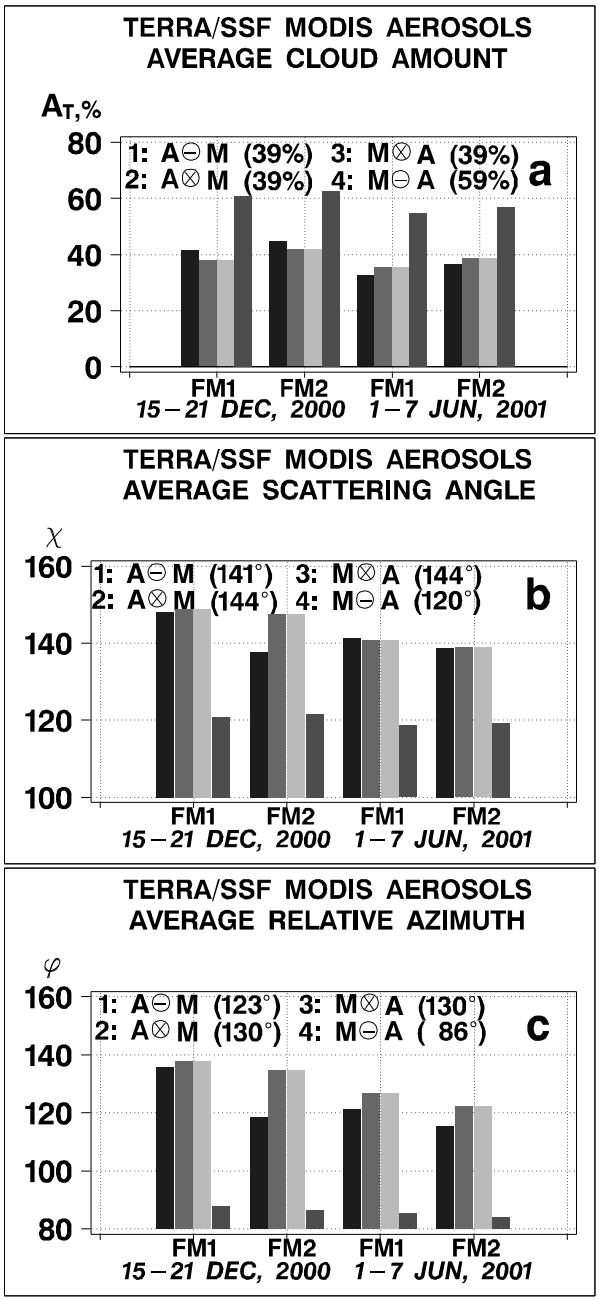


**Fig.4.** Average (a) ambient cloud amount; (b) scattering angle; (c) relative azimuth angle in December 2000 and June 2001, FM1 and FM2 datasets. (Samples defined in caption to Fig.1.)

(E) The FM2 τ-statistics are somewhat higher compared to their FM1 counterparts. The cause for this difference is not entirely clear, but is likely related to sampling as opposed to aerosol algorithm differences.

### *3.3 Possible causes for the sampling M-differences*

Special analyses have shown that geographical differences likely are not the reason for the observed aerosol differences.

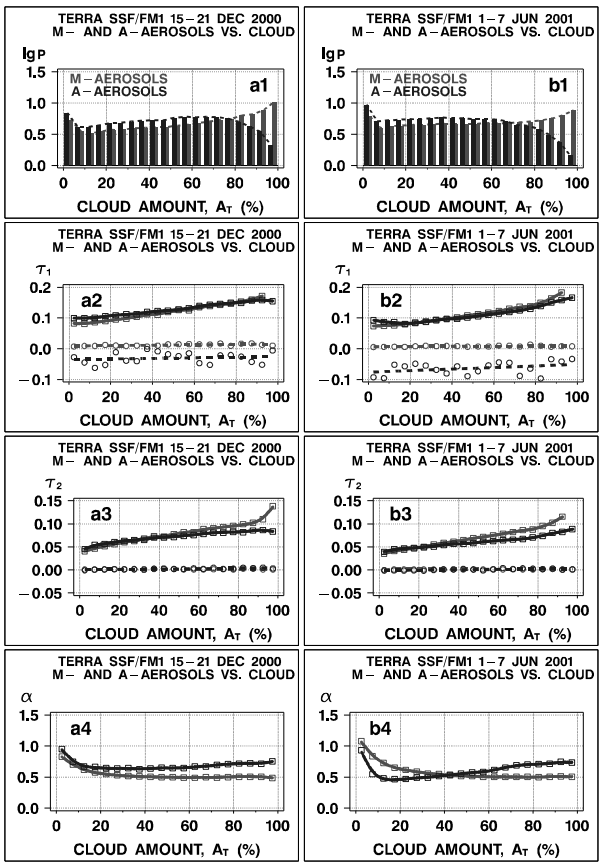


**Fig.5.** (1) Histograms of cloud amount, $A_T$ ($\Delta A_T$=5%), and (2-4) aerosol retrieval trends for (a) December 2000 and (b) June 2001 datasets. (See discussion in section 3.4.)

Figure 4 shows histograms of 3 prominent factors associated with the retrievals: cloud amount in the vicinity of the aerosol retrievals, and two angles (note that the statistics are identical for clusters "2" and "3", which represent different aerosol retrievals in the same MA intersection domain). Three clusters "1"-"3" form a more-or-less uniform group, whereas the M supplement (cluster "4") clearly stands out in all three histograms:
(1) Cloud amount is $A_T$ ~39% in clusters "1"-"3", whereas it is 59% in cluster "4" (note that the $A_T$ is a *conditional* estimate, i.e. only those CERES footprints were used with at least one aerosol retrieval, and that cloud amounts used here come from the A-product).
(2) Relative azimuth angle is ~125° in clusters "1"-"3" compared to ~86° in cluster "4". The relative azimuth cannot be less than 90° in the A-retrievals, which are not produced on the solar side of the orbit, but it may be less than 90° in the M-retrievals.
(3) Scattering angle is ~142° in clusters "1"-"3" versus ~120° in cluster "4".

### *3.4 Cloud Amount Trends in retrievals*

Figures 5a2-a4 and b2-b4 show aerosol retrievals as a function of $A_T$. The trends in τ/α with $A_T$ are strong

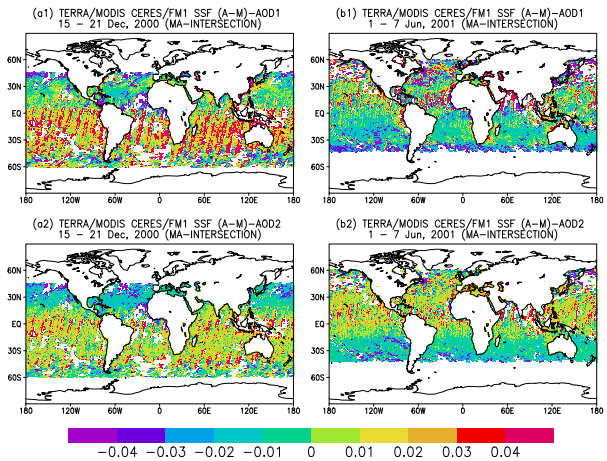


**Fig.6.** Distribution in MA-intersection of (1) $\tau_{1A}$-$\tau_{1M}$, and (2) $\tau_{2A}$-$\tau_{2M}$ derived from *Terra* CERES/FM1 SSF in: (a) December 2000, (b) June 2001. (See discussion in section 3.5.)

in both the M- and A-products. Similar trends have been previously observed in the NOAA/AVHRR and TRMM/VIRS aerosol retrievals (Ignatov et al. 2004bc). The $A_T$-differences between the MA intersection ($A_T$~39%) and the M supplement ($A_T$~59%; cf. Fig.4a) combined with the results in Fig.5 suggest that cloud screening differences between the M- and A-products are the likely cause for the τ-retrieval differences observed in Fig.2. The aerosol-cloud correlations are either "real" (increased hygroscopic aerosol particles that influence cloud formation) or artifacts of the retrievals (residual cloud in a MODIS field-of-view). The increased sensitivity in $\tau_M$ to $A_T$, as compared to sensitivity of $\tau_A$ to $A_T$, suggests that the latter explanation is more likely. However the Ångström exponent trends in Figs.5a4 and b4 are consistent with both hypotheses: α~1 when $A_T$~0%, decreases to α~0.5 at $A_T$~20-40%, and flattens thereafter.

### *3.5 Differences Due to Aerosol Algorithm: Focus on the MA-intersection*

Examination of the effect of M/A-aerosol algorithm differences is best achieved by using the MA intersection, where the effect of sampling is minimized though not removed completely as different MODIS pixels within a CERES FOV could have been used by each algorithm. The respective A-M differences are mapped in Fig.6. The τ-differences, which reach a few hundredths of τ, appear to increase with solar zenith angle and vary with scan position. More analyses are needed to determine if the M, A, or both products are responsible for the patterns. These artifacts may also be related to the aforementioned residual sampling differences. For example, Guzzi et al. (1998) indicate that residual cloud in a sensor FOV may cause artificial sun-angle trends in the retrieved AOD.

In December 2000 (left panels), the biases in τ appear to be quasi-*multiplicative* in both bands, suggesting that they mainly originate from differences

between the M and A aerosol models (e.g. Ignatov and Stowe 2002a), and largely cancel out when their ratio is used to calculate the Ångström exponent. In June 2001, the $\tau_A$-$\tau_M$ differences are smaller, but there is no cancellation in calculating α, indicating the presence of *additive* errors in either $\tau_A$ or $\tau_M$, or both. According to Ignatov (2002), additive errors may be caused by calibration slope uncertainties (Xiong et al. 2002).

### *3.6 December 2000– June 2001 Aerosol Differences*

Consistently with Fig.2, Fig.5 also reveals significant differences between December 2000 and June 2001. In band 1, the minimum in $\tau_A$ is ~-0.04 in December 2000 and decreases to ~-0.07 in June 2001. (Note that negative values of τ are possible in the A-product, whereas the M-product truncates negative retrievals.) Analyses in Ignatov et al. (2004a) suggest that changed radiometric performance of the MODIS instrument in a 5½ month period is a likely cause.

## 4. DISCUSSION AND CONCLUSION

Two aerosol products over oceans available on the *Terra* and *Aqua* CERES SSF datasets reveal common features and some differences, due to different sampling and aerosol algorithms.

The M- and A-product aerosol algorithms differ significantly. The globally invariant aerosol model in the A-product is clearly a limitation, which is purportedly alleviated in the M-product. There are also many non-aerosol factors in the aerosol algorithms (such as the ocean surface reflectance, Rayleigh scattering, gaseous absorption, RTM, and numerical inversion) that are treated differently. Their cumulative result can be assessed only through empirical analyses. The MA intersection sample constructed in this study is best suited to highlight the aerosol algorithm differences. The comparisons demonstrate that aerosol algorithm-induced global differences between the M and A retrievals are within $\sim(4\pm5)\times10^{-3}$ for $\tau_1$, $\sim(3\pm1)\times10^{-3}$ for $\tau_2$, and $\sim(1\pm1)\times10^{-1}$ for α. However, the $\tau_M$-$\tau_A$ - differences appear to be sun-angle and scan-position dependent, and may reach +0.04 in certain domains of sun-view geometries. Some residual sampling discrepancies may still contribute to the observed differences. The aerosol algorithm differences are currently being analyzed in depth and the results will be reported elsewhere.

However, most of the discrepancy between the two products is due to different sampling. The M-products are available in ~90% of the union MA intersection, whereas the A-products occur in only ~55%. Aerosol statistics in the M supplement (M-product only) differs from the MA sample by $\sim+(0.030\pm0.003)$ for both $\tau_1$ and $\tau_2$, and by $\sim-(0.20\pm0.05)$ for α. The A-product differences between the A supplement and MA intersection are statistically insignificant. A possible explanation is related to the fact that aerosol retrievals strongly correlate with the ambient cloud amount in both products although the dependence on cloud amount in the M-product is more pronounced than in the A-product. Similar cloud-aerosol correlations have been observed previously in the NOAA/AVHRR and TRMM/VIRS aerosol retrievals. Drawing a line between the cloud and aerosol is ambiguous. Selecting the thresholds in the cloud screening algorithms is not a completely objective procedure. Note that Myhre et al. (2004) compared five different aerosol products derived from four satellite sensors on three platforms and concluded that the major cause for the observed aerosol differences are likely due to the differences in cloud screening. Further study is needed to resolve these issues. Other reasons for differences between the two aerosol biases are likely related to a different domain of scattering and/or relative azimuth geometries for the samples remaining after cloud and glint screening.

Comparison of the global December 2000 and June 2001 statistics indicate a systematic decrease in aerosol optical depths over the 5½ month period, in both products. The two band τ's analyzed in this study (0.644 and 1.632 μm) change in the same direction but not exactly coherently, leading to opposite trends in the Ångström exponents in the two products: the $\alpha_M$ increases by ~+0.1 whereas the $\alpha_A$ decreases by ~-0.1. Neither of these changes is associated with a significant shift in the geographic or angle domain, or in the cloud amount. Seasonal change, if extant, would be minimal in the most pristine ocean areas, and therefore, is unlikely to affect the minimum in τ. However, the band-1 A-product clearly shows a decline of ~-0.03 in the τ minimum from December 2000 to June 2001. An analysis of band-6 minima is impossible due to radiance truncation. A possible explanation for the change in the minima is the variation in the MODIS performance, which affects the multi-channel M- and the single-channel A-products differently. This example highlights the need for a continuous in-flight monitoring of the performance of all *individual bands* of both MODIS instruments. This should be done as a part of an aerosol quality assurance process as an addition to the MODIS Characterization Support Team tests.

Aerosol retrievals are obtained from the lowest observed radiances, and thus are very sensitive to even the smallest radiometric uncertainties and residual errors of cloud and glint screening. Including single-channel A-type retrievals from each MODIS band used in the standard MOD04 processing would provide an excellent indicator of overall band performance from an aerosol user perspective. Such work should also be closely coordinated with the ocean color retrievals, which are known to be even more demanding to the input data accuracy (G.Feldman and C.McClain, 2004, personal communication). We also recommend an end to the current double truncation of negative radiances on the Level 1B processing and negative aerosol optical depths in the MOD04 processing. Regular (at least one orbit per day) collection of data in the solar reflectance bands on the dark side of the Earth would help to monitor the radiometric performance of the solar reflectance bands (Ignatov 2003). These steps could improve the ability to monitor/diagnose the actual performance of the MODIS instrument in-flight, and greatly facilitate correcting any problems. As an

improvement to the current CERES SSF processing, saving six MODIS radiances used for the MOD04 retrievals over oceans (which are available on MOD04 product) on the SSF datasets would greatly benefit their utility for aerosol analyses and improvements.

Despite some sampling and algorithmic differences, these initial comparisons of the two MODIS-based marine aerosol products indicate that the more spectrally complex MOD04 and simpler AVHRR-type aerosol methods produce relatively consistent results. Although further detailed analyses of the datasets used here and later retrievals will provide information necessary to fully reconcile the discrepancies, it appears that a reliable linkage can be established between the older record based on the simpler methods and the current and future retrievals using more sophisticated approaches. With that connection, it will be possible to establish a trustworthy and valuable long-term climatology of oceanic aerosol properties.

*Acknowledgement.* The MOD04 algorithms were developed in late 1990s by the international team of scientists (NASA/GSFC, USA, and Lab. d'Optique Atmospherique, Univ. of Lille, France) under energetic and enthusiastic leadership of Y.Kaufman. The A-product retrievals were initiated in late 1980s by N.Rao (deceased) and L.Stowe (retired) at NOAA/NESDIS following the pioneering ideas by M.Griggs proposed in mid-1970s. The A-product has been enhanced and applied to other sensor data (TRMM VIRS, and *Terra*/*Aqua* MODIS) under the CERES project. The authors are indebted to J.Xiong, W.Barnes, B.Guenther (NASA/GSFC-MCST), C.Moeller (Univ. Wisconsin, Madison), K.Thome (Univ of Arizona), C.Cao and J.Sullivan (NOAA/NESDIS) for helpful discussions of the MODIS radiometric issues. Help and advice from R.Hucek, S.Mattoo, A.Chu, R.Levy, R.-R.Li, V.Chiang, G.Fireman (NASA/GSFC), Q.Trepte and R.Arduini (NASA/LaRC) is also appreciated. This work was funded under the NASA EOS/CERES (NASA contract L-90987C), the NOAA/NASA/DOD Integrated Program Office, NOAA Ocean Remote Sensing, and Joint Center for Satellite Data Assimilation (NESDIS) Programs. We thank S.Mango (IPO), W.Pichel and F.Weng (NESDIS) for their support and encouragement. The *Terra* CERES SSF data used in this study were obtained from the Atmospheric Sciences Data Center at NASA Langley Research Center. The views, opinions, and findings contained in this report are those of the authors and should not be construed as an official NOAA or U.S. Government position, policy, or decision.

**References**

Ackerman S., et al, 1998: Discriminationg clears-sky from clouds with MODIS. *JGR*, **103**, 32139-32140.

Geier E., et al., 2003: CERES data management system: Single Satellite Footprint TOA/Surface fluxes and clouds (SSF) collection document. Release 2, version 1, 212 pp and appendixes. http://asd-www.larc.nasa.gov/ceres/collect_guide/SSF_CG.pdf

Guzzi R., et al, 1998: GOME cloud and aerosol data products algorithm development. ESA Contract 11572/95/NL/CN, Final Report, 132 p.

Ignatov A., 2002: Sensitivity and information content of aerosol retrievals from AVHRR: Radiometric factors. *Appl.Opt.*, **46**, *6*, 991-1011.

Ignatov A., 2003: Spurious Signals in the TRMM/VIRS Reflectance Channels and their Effect on Aerosol Retrievals. *JTech*, **20**, 1120-1137

Ignatov A., et al, 2004a: Two MODIS aerosol products over ocean on the Terra and Aqua CERES SSF datasets. *JAS*, in press.

Ignatov A., et al, 2004b: Aerosol retrievals from TRMM/ VIRS over open oceans. *JAM*, in prep.

Ignatov A., et al, 2004c: Operational Aerosol Observations (AEROBS) from AVHRR/3 onboard NOAA-KLM satellites. *JTech.*, **21**, 3-26.

Ignatov A., and L.Stowe, 2002a: Aerosol retrievals from individual AVHRR channels: I. Retrieval algorithm and transition from Dave to 6S radiative transfer model. *JAS*, **59**, *3(1)*, 313-334.

Kaufman Y., et al, 1997: Operational remote sensing of tropospheric aerosol over land from EOS/MODIS. *JGR*, **102**, 17,051-17,068.

Levy, R., et al, 2003: Evaluation of the MODIS retrievals of dust aerosol over the ocean during PRIDE. *JGR*, **108**, 8954, 10.1029/2002JD002460.

Martins J., et al, 2002: MODIS cloud screening for remote sensing of aerosols over oceans using spatial variability. *GRL,* **29**, 10.1029/2001GL013252

Minnis, P., et al, 1999: CERES Cloud Properties Derived From Multispectral VIRS Data. *Proc. EOS/SPIE Symposium on Remote Sensing*, **3867***,* Florence, Italy, Sep 20-24, 91-102.

Minnis, P., et al, 2004: Daytime CERES cloud mask for non-polar regions. *JAM*, in prep.

Myhre, G., et al, 2004: Intercomparison of satellite retrieved aerosol optical depth over the ocean. *JAS*, **61**, 499-513.

Remer, L., et al, 2002: Validation of MODIS aerosols over ocean. *GRL*, **29**, 10.1029/2001GL013204.

Remer L., Y. et al, 2004: The MODIS aerosol algorithm, products, and validation. *JAS*, in press.

Tanre, D., et al, 1996: Information on aerosol size distribution contained in solar reflected spectral radiances. *JGR*, **101**, 19,043-19,060.

Tanré D., et al, 1997: Remote sensing of aerosol properties over oceans using the MODIS/EOS spectral radiances. *JGR*, **102**, 16,971-16,988.

Trepte Q., et al., 1999: Scene identification for the CERES cloud analysis subsystem. *Proc. AMS 10th Conf. Atmos. Rad.,* Madison, WI, 169-172.

Wielicki B., et al, 1996: Clouds and the Earth's Radiant Energy System (CERES): An Earth Observing System Experiment. *BAMS*, **77**, *11*, 853-868.

Xiong, J., et al, 2002: MODIS solar reflectance bands calibration algorithm and on-orbit performance. Proc. SPIE - Optical Remote Sensing of the Atmosphere and Clouds III, 4891, 10 pp.